Synthesis of New Lamellar Iron(III) Phosphonates

B. Bujoli,† P. Palvadeau,‡ and J. Rouxel*,‡

Laboratoire de Synthèse Organique, URA CNRS 475, and Institut de Physique et Chimie des Matériaux, UM CNRS 0110, 2, Rue de la Houssinière, 44072 Nantes Cedex 03, France

Received January 26, 1990

The behavior of phenylphosphonic acid toward FeOCl is presented as a pathway for the synthesis of lamellar iron(III) phosphonates, and the following adducts have been isolated: $HFe(C_6H_5PO_3H)_4$ and $HFe(C_6H_5PO_3)_2 \cdot H_2O$. The quasi-one-dimensional structure of $HFe(C_6H_5PO_3H)_4$ has been determined by X-ray crystallography. The crystals are triclinic, space group $P\bar{1}$ with a = 14.968 (9) Å, b = 5.36 (1) Å, c = 8.678 (6) Å, α = 88.5 (1)°, β = 86.41 (6)°, γ = 89.6 (1)°, V = 694 (1) Å^3, Z = 1. The final R and R_w values were 0.063 and 0.068, respectively. In acetone or toluene this kinetic compound gradually turns into $HFe(C_6H_5PO_3)_2 \cdot H_2O$ for which a structure close to that of α-ZrP is proposed. Three crystallographic forms of $HFe(C_6H_5PO_3)_2 \cdot H_2O$ have been obtained, differing from each other in the location of the water molecule in the layered structure.

Introduction

Various metal phosphonates have been described for their applications in agriculture,[1,2] catalysis,[3,4] sorption of heavy metals in solution,[5] etc. Special interest is given to layered phosphonates with alternating organic and inorganic layers in which a large range of organic groups are covalently appended on both sides of the sheets, thus providing an ordered disposition of sites within them. In fact, if a layered solid can be synthesized, presenting sites accessible to exterior species via intercalation, one might expect enhanced selectivity for certain reactions in relation with the geometry of the sites and their chemical environment.[6] Good examples are zirconium phosphate and related organophosphonates of tetravalent metals that are widely used for their intrinsic catalytic properties or their ability to fix metal complexes to produce immobilized "homogeneous catalysts".[3,4,7,8] Such compounds are usually obtained by precipitating phosphonates with M^{4+} ions.[9-12] Many investigations have been reported[13-19] concerning the lamellar iron oxychloride, consisting of slabs built up of two alternate metal oxygen layers sandwiched between two layers of labile chlorine atoms. An interesting feature of this compound is the possibility of manipulation of its surface textural properties by variation of the pendant groups via topochemical graftings.[19c,20] Our approach in this work has been to prepare lamellar derivatives of FeOCl by anchoring organophosphonates onto the FeO double layer, with retention of the intercalation properties of the pristine material. This should still allow further reactions in the constrained van der Waals gap. This paper deals with the action of phosphonic acids with FeOCl as a new route to lamellar iron phosphonates.[21] Phenylphosphonic acid has been selected to carry out a systematic study of the influence of various parameters (solvent, concentration, time of reaction, etc.) on the reaction process for which the different steps are discussed.

Experimental Section

Reagents. Iron(III) oxychloride was prepared from Fe_2O_3 and $FeCl_3$ by the usual sealed-tube technique.[22] Phenylphosphonic acid and solvents were of reagent grade quality and were obtained from MERCK (Uvasol).

Preparation of Compounds. $HFe(C_6H_5PO_3H)_4$: A typical reaction procedure consisted of sealing 107 mg (1 mmol) of FeOCl, 790 mg (5 mmol) of phenylphosphonic acid, and 5 mL of dry dichloromethane in a Pyrex tube (15 cm in length × 1 cm in diameter) and heating the mixture at 80 °C for 24 h. The white crystalline product was filtered off with suction, rinsed with

Table I. Crystallographic Data for $HFe(C_6H_5PO_3H)_4$

$C_{24}H_{25}O_{12}P_4Fe$	T = 23 (1) °C
a = 14.968 (9) Å	λ = 0.710 69 Å
b = 5.36 (1) Å	ρ_{calcd} = 1.64 g·cm^{-3}
c = 8.678 (6) Å	μ = 71.55 cm^{-1}
α = 88.5 (1) °	scan type = $\omega/2\theta$
β = 86.41 (6) °	scan width, deg = 1.2 + 0.8 tan θ
γ = 89.6 (1) °	data coll range (θ) = 1.5-30°
V = 694 (1) Å^3	($h = \bar{2}4$-24, k = 0-8, $l = \bar{1}3$-13)
Z = 1	$R = \sum\|\|F_o\| - \|F_c\|\|/\sum\|F_o\|$ = 0.063
fw = 685.20	$R_w = [\sum(\|F_o\| - \|F_c\|)^2/\sum w\|F_o\|^2]^{1/2}$ = 0.068
space group = $P\bar{1}$ (No. 1)	

†Laboratoire de Synthèse Organique.
‡Institut de Physique et Chimie des Matériaux.
*Author to whom correspondence should be addressed.

(1) (a) Chalandon, A.; Crisinel, P.; Horrière, D. Beach, B. G. W. *Proc. Br. Crop Prot. Conf.—Pests Dis.* **1979**, *2*, 347. (b) Bompeix, G.; Saindrenan, P.; Mourichon, X.; Chalandon, A. *Proc. Br. Crop Prot. Conf.—Pests Dis.* **1979**, *1*, 87.

(2) Kodama, Y.; Kodama, T.; Nakabayashi, M.; Senoura, M.; Kiba, Y. Japan Patent No. 7703024; class. No. C07F9/40; Appl./Priority No. 75/79351; June 27, 1975.

(3) King, D. L.; Cooper, M. D.; Faber, M. A.; Schramm, C. M. Catalytica Report, Molecularly Engineered Layered Structures: Novel materials for catalysis and surface chemistry, 1988.

(4) (a) DiGiacomo, P. M.; Dines, M. B. *Polyhedron* **1982**, *1*, 61. (b) DiGiacomo, P. M.; Dines, M. B.; Parziale, V. E. Eur. Patent No. 10366; class. No. C07F9/09; Appl./Priority No. 945971; Sept 26, 1978.

(5) Tsvetaeva, N. E.; Rudaya, L. Ya.; Fedoseev, D. A.; Ivanova, L. A.; Shapiro, K. Yu. U.S.S.R. Patent No. 623392; class. No. C22B60/02; Appl./Priority No. 2377581; June 28, 1976.

(6) Such effects have been seen in clays. See: Pinnavaia, T. J.; Raythatha, R.; Lee, J. G.; Halloran, L. J.; Hoffman, J. F. *J. Am. Chem. Soc.* **1979**, *101*, 6891.

(7) (a) Lane, R. H.; Callahan, K. P.; Cooksey, R.; DiGiacomo, P. M.; Dines, M. B.; Griffith, P. C. *Prepr.—Am. Chem. Soc., Div. Pet. Chem.* **1982**, *27*(3), 624. (b) Callahan, K. P.; DiGiacomo, P. M.; Dines, M. B. U.S. Patent No. 4386013; class. No. 252-431P, B01J31/24; Appl./Priority No. 295340; Aug 24, 1981. (c) Dines, M. B.; DiGiacomo, P. M.; Callahan, K. P. U.S. Patent No. 4 384981; class. No. 252-431N, B01J31/22; Appl./Priority No. 295341; Aug 24, 1981.

(8) (a) Johnson, J. W.; Jacobson, A. J.; Brody, J. F.; Lewandowski, J. T. *Inorg. Chem.* **1984**, *23*, 3842. (b) Johnson, J. W.; Jacobson, A. J.; Butler, W. M.; Rosenthal, S. E.; Brody, J. F.; Lewandowski, J. T. *J. Am. Chem. Soc.* **1989**, *111*, 381.

(9) Mikulski, C. M.; Karayannis, N. M.; Minkiewicz, J. V.; Pytlewski, L. L.; Labes, M. M. *Inorg. Chim. Acta* **1969**, *3*, 523.

(10) Yamanaka, S. *Inorg. Chem.* **1976**, *15*, 2811.

(11) (a) Alberti, G.; Constantino, U.; Alluli, S.; Tomassini, J. *J. Inorg. Nucl. Chem.* **1978**, *40*, 1113. (b) Alberti, G.; Constantino, U.; Giovagnotti, M. L. L. *J. Chromatogr.* **1979**, *180*, 45. (c) Casciola, M.; Constantino, U.; Fazzini, S.; Tosoratti, G. *Solid State Ionics* **1983**, *8*, 27.

(12) (a) Dines, M. B.; DiGiacomo, P. M. *Inorg. Chem.* **1981**, *20*, 92. (b) Dines, M. B.; DiGiacomo, P. M.; Callahan, K. P.; Griffith, P. C.; Lane, R.; Cooksey, R. E. In *Chemically Modified Surfaces in Catalysis and Electrocatalysis*; Miller, J., Ed.; ACS Symposium Series 192; American Chemical Society: Washington, DC, 1982; p 223. (c) Dines, M. B.; Griffith, P. C. *Inorg. Chem.* **1983**, *22*, 567. (d) Dines, M. B.; Cooksey, R. E.; Griffith, P. C. *Inorg. Chem.* **1983**, *22*, 1003. (e) Dines, M. B.; Griffith, P. C. *Polyhedron* **1983**, *2*, 607.

0897-4756/90/2802-0582$02.50/0

acetone, and dried at room temperature under vacuum, yield 85%. Anal. Calcd for $C_{24}H_{25}O_{12}P_4Fe$: C, 42.05; H, 3.65; P, 18.11; Fe, 8.15. Found: C, 41.91; H, 3.62; P, 18.19; Fe, 8.24.

$HFe(C_6H_5PO_3)_2 \cdot H_2O$, α-phase: A mixture of 107 mg of FeOCl and 316 mg (2 mmol) of phenylphosphonic acid in 25 mL of dry acetone was refluxed in a round-bottom flask under nitrogen and stirred for 20 h. The product was isolated by filtration as a white precipitate in 85% yield, washed with acetone, and dried under vacuum. Anal. Calcd for $C_{12}H_{13}O_7P_2Fe$: C, 37.24; H, 3.38; P, 16.00; Fe, 14.42. Found: C, 37.16; H, 3.38; P, 15.95; Fe, 14.27.

$HFe(C_6H_5PO_3)_2 \cdot H_2O$, β-phase: The same procedure as above, using toluene instead of acetone, gave the β-phase as a white solid, yield 90%. Anal. Calcd for $C_{12}H_{13}O_7P_2Fe$: C, 37.24; H, 3.38; P, 16.00; Fe, 14.42. Found: C, 37.32; H, 3.34; P, 16.08; Fe, 14.54. This phase can be prepared as well in acetone, but in this case we cannot avoid the presence of small amounts of the γ-phase in the final product.

$HFe(C_6H_5PO_3)_2 \cdot H_2O$, γ-phase: The FeOCl/phenylphosphonic acid (1:2) mixture and 5 mL of dry acetone were sealed in a Pyrex tube and heated at 80 °C for 4 days. The product was a white solid, yield 70%. Anal. Calcd for $C_{12}H_{13}O_7P_2Fe$: C, 37.24; H, 3.38; P, 16.00; Fe, 14.42. Found: C, 37.30; H, 3.40; P, 16.11; Fe, 14.42.

Physical Methods. The infrared absorption spectra (4000–400 cm^{-1}) were obtained by using a FTIR Nicolet 20SX spectrometer with the usual KBr pellet technique. ^{57}Fe Mössbauer spectra of powder samples, with radiation from ^{57}Co in Pd metal, were measured at room temperature with a constant-acceleration automatic-folding Elscint spectrometer. The susceptibility measurements were performed with powder samples on a Faraday balance described earlier[18] in the temperature range 4.2–300 K. Powder X-ray diffraction patterns were obtained by using a Siemens diffractometer with Cu Kα radiation. The samples were mounted on glass slides by using double-sided cellophane tape. A Jeol JM-35C equipped with a Tracor TN5500 microZ system was used for X-ray microanalyses (energy dispersive spectroscopy) of powder samples for the kinetics studies. Iron, phosphorus, carbon and hydrogen analyses of pure samples of compounds I and II (α, β, γ) were performed by the CNRS Analysis Laboratory, Vernaison. The thermogravimetric analyses were carried out on a Setaram TG-DTA92 thermogravimeter analyzer fitted with a Balzers QMG420 mass spectrometer.

Crystal Structure Determination. Single crystals of $HFe(C_6H_5PO_3H)_4$ were obtained by using the procedure described above. The crystal parameters and other interesting data are summarized in Table I. The crystal used was a clear, colorless needle of dimensions 0.06 × 0.07 × 0.36 mm.

Data were collected on an Enraf-Nonius CAD4 diffractometer using Mo Kα radiation (λ = 0.71069 Å) with a graphite monochromator. Cell constants on an orientation matrix for data collection were obtained from least-squares refinement, with use of the setting angles of 19 reflections in the range $2° < \theta < 25°$. To check on crystal and instrument stability, three representative reflections were measured every 60 min and no decay was observed. For $HFe(C_6H_5PO_3H)_4$, the calculated linear absorption coefficient μ was 71.55 cm^{-1}, and since the crystal was very small, no absorption correction was applied. A secondary extinction correction was applied.[23] The final coefficient, obtained by least-squares refinement, was 2.7 (5) × 10^{-7} (in absolute units). Reflections with $I > 3\sigma(I)$ (758 reflections) were used for the structure refinement. All calculations were done using the SDP-PLUS program (1982 version) written by Frenz.[24]

Laue symmetry with no systematically absent reflections were consistent with triclinic space group $P1$ and $P\bar{1}$. Refinement was begun in $P1$ and showed that Fe was an inversion center. Thus, the structure was determined in the $P\bar{1}$ space group. By symmetry,

Table II. Positional Parameters and B_{eq} Values[a] for the Non-Hydrogen Atoms of $HFe(C_6H_5PO_3H)_4$

atom	x	y	z	B, Å²
Fe	−0.0042 (6)	0.013 (2)	0.007 (1)	1.08 (5)*
P(1)	0.1117 (3)	0.4723 (8)	0.1310 (5)	1.59 (8)
P(2)	0.1108 (3)	0.1312 (8)	0.6622 (5)	1.80 (8)
O(1)	0.0982 (6)	0.223 (2)	0.053 (1)	1.9 (2)
O(2)	0.0667 (6)	0.460 (2)	0.303 (1)	1.9 (2)
O(3)	0.0761 (6)	−0.295 (2)	0.054 (1)	1.9 (2)
O(4)	0.0776 (7)	0.081 (2)	0.500 (1)	2.0 (2)
O(5)	0.0551 (6)	−0.016 (2)	−0.216 (1)	1.8 (2)
O(6)	0.1101 (7)	0.422 (2)	0.688 (1)	2.4 (2)
C(1)	0.231 (1)	0.501 (3)	0.152 (2)	1.8 (3)*
C(2)	0.260 (1)	0.694 (3)	0.244 (2)	2.9 (4)*
C(3)	0.353 (1)	0.718 (4)	0.268 (2)	4.1 (4)*
C(4)	0.412 (1)	0.547 (4)	0.195 (2)	3.8 (4)*
C(5)	0.383 (1)	0.352 (4)	0.106 (2)	3.6 (4)*
C(6)	0.291 (1)	0.324 (3)	0.086 (2)	3.3 (4)*
C(7)	0.228 (1)	0.062 (3)	0.666 (2)	1.9 (3)*
C(8)	0.290 (1)	0.220 (3)	0.581 (2)	3.3 (4)*
C(9)	0.384 (1)	0.165 (4)	0.598 (2)	4.1 (4)*
C(10)	0.411 (1)	−0.028 (4)	0.686 (2)	4.2 (4)*
C(11)	0.351 (1)	−0.180 (4)	0.769 (2)	4.1 (4)*
C(12)	0.257 (1)	−0.142 (3)	0.760 (2)	2.9 (4)*

[a] Starred values denote atoms refined isotropically. Anisotropically refined atoms are given in the form of the isotropic equivalent displacement parameter defined as $^4/_3[a^2B_{11} + b^2B_{22} + c^2B_{33} + ab(\cos\gamma)B_{12} + ac(\cos\beta)B_{13} + bc(\cos\alpha)B_{23}]$.

Table III. Selected Bond Lengths (Å) and Bond Angles (deg) for $HFe(C_6H_5PO_3H)_4$[a]

1	2	3	1–2	1–2–3
O1	Fe	O1[a]	1.97 (1)	173.7 (5)
O1	Fe	O3		93.4 (5)
O1	Fe	O_3[a]		87.2 (4)
O1	Fe	O5		87.2 (4)
O1	Fe	O5[a]		93.4 (5)
O1[a]	Fe	O3	2.00 (1)	90.8 (5)
O1[a]	Fe	O3[a]		88.2 (5)
O1[a]	Fe	O5		88.0 (5)
O1[a]	Fe	O5[a]		91.0 (5)
O3	Fe	O3[a]	1.93 (1)	175.5 (6)
O3	Fe	O5		91.8 (5)
O3	Fe	O5[a]		92.4 (5)
O3[a]	Fe	O5	2.08 (1)	83.7 (4)
O5	Fe	O3[a]	1.92 (1)	92.0 (5)
O5	Fe	O5[a]	2.08 (1)	175.7 (6)
O1	P1	O2	1.535 (7)	109.6 (4)
O1	P1	O3[b]		117.5 (5)
O1	P1	C1		106.6 (5)
O2	P1	O3[b]s	1.598 (7)	106.9 (4)
C1	P1	O2	1.81 (1)	105.5 (4)
O3[b]	P1	C1	1.506 (7)	110.2 (4)
O4	P2	O5[c]	1.554 (7)	109.8 (4)
O4	P2	O6		109.0 (4)
O4	P2	C7		110.3 (4)
O5[c]	P2	O6	1.512 (7)	113.9 (4)
C7	P2	O5[c]	1.79 (1)	112.5 (4)
O6	P2	C7	1.580 (7)	101.0 (4)

[a] Symmetry operators: (a) $-x, -y, -z$; (b) $x, 1 + y, z$; (c) $x, y, 1 + z$; (d) $-x, 1 - y, 1 - z$.

(13) (a) Kanamaru, F.; Shimada, M.; Koizumi, M.; Takano, M.; Takada, M. *J. Solid State Chem.* **1973**, *7*, 297. (b) Kikkawa, S.; Kanamaru, F.; Koizumi, M. *Inorg. Chem.* **1976**, *15*, 2195.
(14) Halbert, T. R.; Scanlon, J. C. *Mater. Res. Bull.* 1979, *14*, 415.
(15) Herber, R. H.; Maeda, Y. *Physica B + C (Amsterdam)* **1981**, *105*, 243.
(16) Kauzlarich, S. M.; Teo, B. K.; Averill, B. A. *Inorg. Chem.* **1986**, *25*, 1209.
(17) Weiss, A.; Choy, J. H. *Z. Naturforsch.* **1984**, *39b*, 1193.
(18) Maguire, J. A.; Banewicz, J. J. *Mater. Res. Bull.* **1984**, *19*, 1573.
(19) (a) Hagenmuller, P.; Portier, J.; Barbe, B.; Bouclier, P. *Z. Anorg. Allg. Chem.* **1967**, *355*, 209. (b) Armand, M.; Coic, L.; Palvadeau, P.; Rouxel, J. *J. Power Sources* **1978**, *3*, 137. (c) Villiéras, J.; Chiron, R.; Palvadeau, P.; Rouxel, J. *Rev. Chim. Minér.* **1985**, *22*, 209.
(20) Kikkawa, S.; Kanamaru, F.; Koizumi, M. *Inorg. Chem.* **1980**, *19*, 259.
(21) Palvadeau, P.; Queignec, M.; Venien, J. P.; Bujoli, B.; Villiéras, J. *Mater. Res. Bull.* **1988**, *23*, 1561.
(22) Schafer, H. *Z. Anorg. Allg. Chem.* **1949**, *260*, 279.
(23) Zachariasen, W. H. *Acta Crystallog.* **1963**, *16*, 1139.
(24) Frenz, B. A. *Enraf-Nonius Structure Determination Package*; Delft University Press: Delft, Holland, 1982.

Table IV. Kinetic Data for the $C_6H_5PO_3H_2$/FeOCl Reaction in Various Solvents

	group 1	group 2	group 3
solvent	dichloromethane toluene hexane	acetonitrile acetone tetrahydrofuran	water ethyl alcohol
progress of the reaction	very rapid complete disappearance of FeOCl in 5 h for toluene and hexane and only 30 min for CH_2Cl_2	slow complete disappearance of FeOCl for all three solvents in 24–48 h	very slow incomplete reaction even after 2 weeks

Fe is forced to lie on an inversion center. The P positions were determined from a Patterson map, and the remaining non-H atoms were located in succeeding difference Fourier syntheses. The structure was refined by full-matrix least-squares procedures with anisotropic thermal parameters for P and O atoms. Fe is located close to the origin for which the symmetry of site is $\bar{1}$. Thus this atom statistically occupies at 50% an off-center position in its coordination octahedron. Fe could not be refined anisotropically and was refined isotropically along with C atoms. Some of the hydrogen atoms were located from ΔF map but not refined in order to keep a data to parameter ratio higher than 6:1. $\sum w(|F_o| - |F_c|)^2$ was minimized, and the weight of each reflection was calculated as $w = 1/(1 + [(F_o - F_{av})/F_{max}]^2)$. The atomic scattering factors were taken from the usual tabulation,[25] and the effects of anomalous dispersion were included in F_c.[26] Refined positional parameters for non-hydrogen atoms and main bond distances and angles are given in Tables II and III, respectively.

Results and Discussion

Significant differences in the reactivity of phenylphosphonic acid toward FeOCl were observed, depending on the nature of the solvent used, all other conditions being equal. The solvents were classified into three groups that exhibited different rates for the consumption of iron oxychloride, which was easily observed due to a color change in the starting material from reddish violet to white.

The amount of chlorine present in the isolated solid sample was measured by X-ray fluorescence in order to determine the proportion of FeOCl that did not react. These results are reported in Table IV. Because the solvents in group 3 (water, ethanol) led to incomplete reactions, dichloromethane, toluene, and acetone, affording different kinetics of reaction, were selected for the rest of our study.

Since phenylphosphonic acid is much less soluble in the solvents of group 1 than in those of groups 2 and 3, the observed reaction rates can be rationalized by decreased association with the solvent, resulting in increased accessibility to its reactive groups (phosphoryl group P=O and acidic OH) and increased rate of complex formation. The opposite phenomenon is observed as the solvation improves, in the order water > ethyl alcohol > acetone. In dichloromethane, hexane, and toluene, phenylphosphonic acid dissolves only as fast as it is consumed, but this process does not seem to affect the reaction kinetics. When the molar ratio (S) of phenylphosphonic acid to iron oxychloride was allowed to vary with all other parameters fixed, two compounds were obtained: $HFe(C_6H_5PO_3H)_4$ (I) and $HFe(C_6H_5PO_3)_2{\cdot}H_2O$ (II). The chemical formula of II was evaluated by elemental analyses.

In the three solvents studied, when S was close to 2, only phases of type II were produced whereas the reaction yielded I when S was greater than or equal to 4 (eqs 1 and 2).

Table V. Dependence of the Proportion of Compounds I and II versus S in Dichloromethane

	S = 2.5	S = 3	S = 3.5
% of I	20	45	70
% of II	80	55	30

$$S = 2 \quad FeOCl + 2C_6H_5PO(OH)_2 \rightarrow HFe(C_6H_5PO_3)_2{\cdot}H_2O + HCl \quad (1)$$

$$S \geq 4 \quad FeOCl + 4C_6H_5PO(OH)_2 \rightarrow HFe(C_6H_5PO_3H)_4 + H_2O + HCl \quad (2)$$

In the intermediate cases ($2 < S < 4$), a competition between the formation of both species was observed. The room-temperature Mössbauer spectra of the isolated products are well described by the overlap of two symmetric doublets with intensities indicative of the proportion of each component. The isomer shifts of the two doublets are 0.44 (I) and 0.47 mm/s (II), and the quadrupole splittings 0.30 (I) and 0.40 mm/s (II). After deconvolution the contribution of each doublet is estimated (Table V).

When the reaction time was prolonged beyond the duration necessary for the complete consumption of iron oxychloride ($S > 4$), $HFe(C_6H_5PO_3H)_4$ evolved in the medium, leading to compounds of type II, with a rate of conversion dependent upon the nature of the solvent. This conversion is complete in acetone (rapid) and toluene (slow) but nonexistent in dichloromethane. On the other hand ($S = 2$), three phases α, β, and γ, with identical compositions, $HFe(C_6H_5PO_3)_2{\cdot}H_2O$, but different X-ray, IR, and Mössbauer spectra were detected during the reaction. These are discussed in more detail below. The transition from I to II with simultaneous evolution of two phosphonic groups (eq 3) is favored as the latter are soluble in the reaction mixture (case of acetone).

$$\underset{I}{HFe(C_6H_5PO_3H)_4} + H_2O \rightarrow \underset{II}{HFe(C_6H_5PO_3)_2{\cdot}H_2O} + 2C_6H_5PO_3H_2 \quad (3)$$

On the other hand, the fixation of one water molecule by I is likely to be favored if the miscibility of water with the solvent used is good (case of acetone and toluene). Consequently, phase I appears to be a kinetic product, forming for stoichiometries greater than 2 and showing a stability dependence on the solvent used. It is worth noting that compound I, isolated, soaked in acetone with 2 equiv of phosphonic acid, and heated at 80 °C leads, in a few hours, to materials of type II that seem therefore to be thermodynamically stable phases.

Structure of Compound I. Positional parameters are given in Table II, and selected bond distances and angles are listed in Table III. Figures 1 and 2 show that the structure is layered and that the metal atoms are coplanar.

(25) Cromer, D. T.; Waber, J. T. *International Tables for X-Ray Crystallography*; Kynoch: Birmingham, England, 1974; Vol. IV, Table 2.2B.

(26) Cromer, D. T.; Ibers, J. A. *International Tables for X-Ray Crystallography*; Kynoch: Birmingham, England, 1974; Vol. IV, Table 2.3.1.

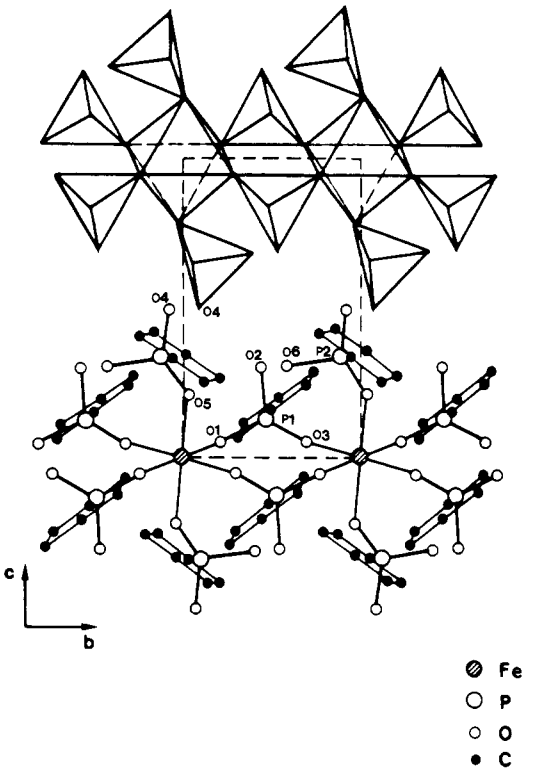

Figure 1. Structure of $HFe(C_6H_5PO_3H)_4$ viewed down the *a* (stacking) axis.

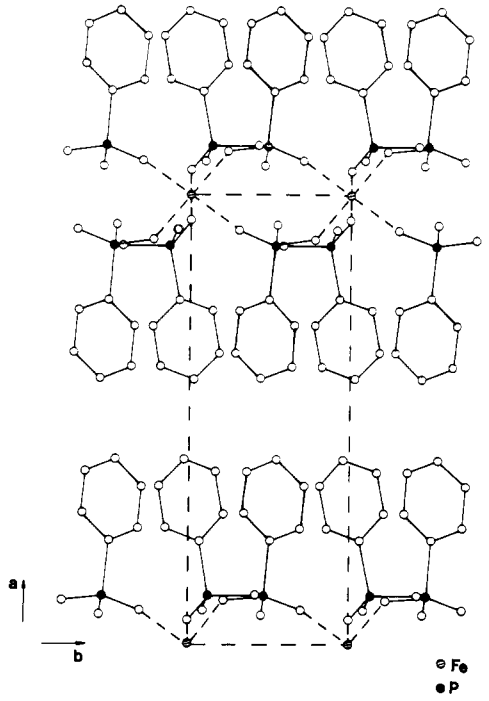

Figure 2. Structure of $HFe(C_6H_5PO_3H)_4$ viewed down the *c* axis.

In $HFe(C_6H_5PO_3H)_4$ the FeO_6 octahedra and $PO_3C_6H_5$ tetrahedra are arranged in infinite chains running parallel to the *b* axis. Each FeO_6 octahedron is connected to six different phosphonate groups, four of which bridge two iron atoms through two of its oxygens and the two others bond to only one Fe atom.

This material has a quasi-one-dimensional structure along the *b* axis; the distance between two neighboring metals along this direction is 5.36 Å, close to the value of 5.29 Å observed in the α-ZrP structure for two zirconium atoms linked by O–P–O bridges.[27] The P–C bond points toward an adjacent sheet of the structure, and the phenyl groups make van der Waals contacts between these layers (*a* axis). The cohesion of the network along the *c* axis is provided by hydrogen bonds through the interagency of the unshared oxygen vertices of tetrahedra, which presumably bear the hydrogen atoms.

Table VI. Possible Hydrogen Bond Distances (Å) in $HFe(C_6H_5PO_3H)_4$[a]

O4–O4[a]	2.48 (1)	O2–O6[d]	2.71 (1)
O4–O2	2.63 (1)		

[a] Symmetry operators: (*a*) $-x, -y, -z$; (*d*) $-x, 1-y, 1-z$.

After refinement of the non-H atoms, a Fourier difference map was computed that revealed, among peaks corresponding to hydrogens belonging to the aromatic rings, two peaks allowing location of one hydrogen close to O4 (H1) and the other next to O6 (H2). In the case of O1, O3, and O5, the P–O distances range from 1.50 to 1.53 Å and are consistent with values previously observed for phosphorus atoms bearing oxygens bonded to a metallic nucleus.[27,28] The P1–O2 and P2–O6 distances are significantly longer (~1.60 Å) and correspond to POH groups. Four of the nonaromatic hydrogens (H2 and H3) are linked to O6 and O2, respectively (centrosymmetric group). Finally, an intermediate distance is observed for P2–O4, and the position of H1 (close to O4) given from the Fourier difference map is located on an inversion center (0.02, 0.04, 0.52) which is reasonable, taking into account that there is an odd number of hydrogen atoms per empirical formula weight and that the space group is centrosymmetric. The fact that the O4–O4 distance is short (2.48 Å) leads us to assume that the H1 atom lies between two O4 oxygens with relatively strong hydrogen bonding as reported by Oyetola[29] in the neutron diffraction study of $HTa(PO_4)_2$ and by Philippot[30] for $KH_5(PO_4)_3$.

The other oxygen–oxygen distances range from 2.55 to 3.15 Å (Table VI) and suggest probable hydrogen bonding between atoms H2 and H3 and neighboring oxygens, with a force depending on these oxygen–oxygen distances and nonlinear or out-of-plane OH···O configurations, accounting for the large distribution of the O–H stretching vibrations (2800–3450 cm^{-1}) observed by infrared spectroscopy.[31,32]

Compounds II, α, β, and γ Phases. As mentioned previously, $HFe(C_6H_5PO_3)_2 \cdot H_2O$ was detected as three structural forms, α, β, and γ. These phases formed in a precise order, independent of the nature of the solvent. The only parameter governing this process was the duration of the reaction according to eq 4.

$$FeOCl + 2C_6H_5PO_3H_2 \xrightarrow{t_1} \underset{\alpha}{HFe(C_6H_5PO_3)_2 \cdot H_2O} \xrightarrow{t_2} \underset{\beta}{HFe(C_6H_5PO_3)_2 \cdot H_2O} \xrightarrow{t_3} \underset{\gamma}{HFe(C_6H_5PO_3)_2 \cdot H_2O} \quad (4)$$

If all experimental parameters were fixed, (except the amount of solvent), dilution slowed down the transitions $\alpha \rightarrow \beta \rightarrow \gamma$. If the experimental procedure was modified by using sealed glass tubes instead of a flask with mere reflux of the solvent at ambient pressure, the process

(27) (a) Clearfield, A.; Smith, G. D. *Inorg. Chem.* **1969**, *8*, 431. (b) Clearfield, A.; Troup, J. M. *Inorg. Chem.* **1977**, *16*, 3311.
(28) Cao, G.; Lee, H.; Lynch, M. V.; Mallouk, T. E. *Inorg. Chem.* **1988**, *27*, 2781.
(29) Oyetola, S. Ph.D. Thesis, Nantes University, June 1988.
(30) Philippot, E.; Richard, P.; Roudault, R.; Maurin, M. *Rev. Chim. Minér*, **1972**, *9*, 825.
(31) Secco, E. A.; Worth, G. G. *Can. J. Chem.* **1987**, *65*, 2504.
(32) Novak, A. *Struct. Bonding* **1974**, *18*, 177.

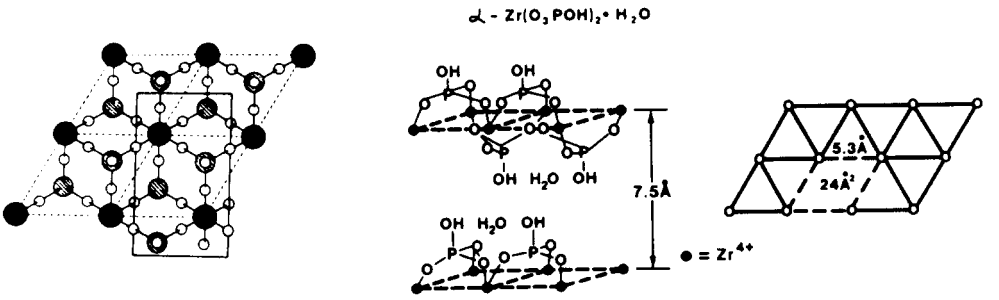

Figure 3. α-ZrP structure.

Table VII. X-ray Powder Data for α, β, and γ

	α phase			β phase			γ phase							
D, Å	15.0 (001)	7.50 (002)	5.0 (003)	14.66 (001)	7.33 (002)	4.87 (003)	15.11 (001)	7.56 (002)	5.04 (003)	4.70	4.41	3.92	3.78 (004)	3.02 (005)
I, %	100	8	6	100	12	8	100	16	13	5	4	2	5	3

speeded up. Finally, if the solvent was changed, the rate of $\alpha \rightarrow \beta \rightarrow \gamma$ transitions increased on passing from acetone to toluene to dichloromethane. Exploiting the above three parameters, it was possible to optimize the times t_1, t_2, and t_3 in order to isolate each of the phases with a very good purity (see Experimental Section).

Characterization of Phases α, β, and γ. The three $HFe(C_6H_5PO_3)_2 \cdot H_2O$ phases are likely based on the $Zr(PO_3R)_2$ structure, which can be synthesized according to eq 5,[3,11a] close to the route starting with iron oxychloride (eq 6):

$$M^{IV}OX_2 + 2RPO_3H_2 \rightarrow M(RPO_3)_2 + 2HX + H_2O \quad (5)$$

$$FeOCl + 2RPO_3H_2 \rightarrow HFe(RPO_3)_2 \cdot H_2O + HCl \quad (6)$$

The structure of α-ZrP ($Zr(PO_4H)_2 \cdot H_2O$) was determined in 1969 by Clearfield[27] (Figure 3).

The metallic nuclei occupy the apices of a pseudohexagonal arrangement, each Zr atom being octahedrally coordinated to oxygens belonging to six different phosphate tetrahedra. The octahedra are linked by O–P–O bridges of phosphate groups located above and below the metallic atom planes; the remaining hydroxyl groups are directed perpendicular to those planes. A similar structure has been reported by Pannetier et al.[33] for $Rb^{I}Tl^{III}(SO_4)_2$. When phosphonic acids were used according to eq 5 (R = organic group), structures related to α-ZrP model were obtained in which the hydroxyl groups were replaced by organic substituents. Single crystals of a suitable size for determining the crystal structure of compounds α, β, and γ by X-ray procedures were not obtained. However, to support our assumptions, several investigations capable of giving indirect information on the crystalline structure of these compounds were undertaken. In the three cases, the products as white semicrystalline solids gave X-ray powder patterns exhibiting a prominent series of *h*00 diffraction peaks (with enhanced intensities resulting from preferred orientation), indicative of a layered compound where *a* is the stacking axis (see Table VII).

It was then possible to infer that the interlayer distance *a* was about 15 Å, equal to the *d* spacing given in the literature for $Zr(C_6H_5PO_3)_2$[12a] and consistent with the value of 14.97 Å measured for $HFe(C_6H_5PO_3H)_4$, whose structure is close to that of α-ZrP. In addition, we have shown that compound I was a precursor to compounds II via a transition apparently involving a contraction of $HFe(C_6H_5P-O_3H)_4$ with concomitant evolution of phosphonic acid and change from a quasi-one-dimensional to a bidimensional structure. In fact, if the layers are shifted in the (*b*,*c*) plane along a gliding vector $\vec{v}$, with elimination of monodentate phosphonate groups, a structure close to that of α-ZrP is obtained (Figure 4).

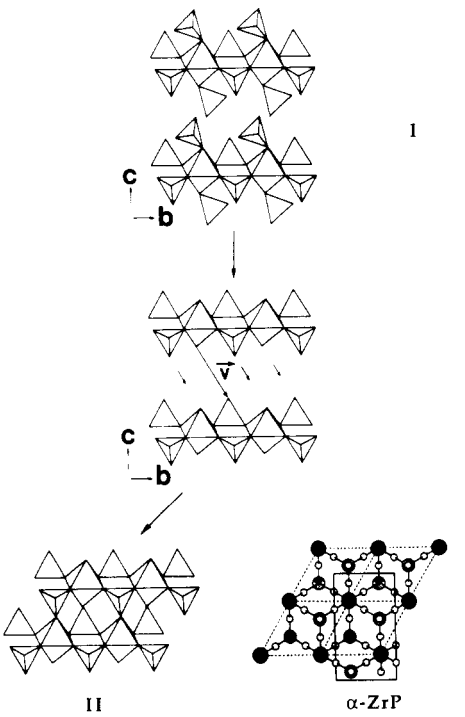

Figure 4. Schematic illustration of the possible transition from I to II.

In other words, it seems likely that α, β, and γ also have layered structures in which the intralayer structural features are essentially the same as those in the α-ZrP structure but with two phosphonate anions probably connected by a weak hydrogen bond as in $HNd(PO_3H)_2 \cdot 2H_2O$.[34] Room-temperature Mössbauer and infrared spectra of α, β, and γ are shown in Figure 5.

The Mössbauer spectra of α, β, and γ show nearly identical isomer shifts (0.43–0.45 mm/s) that are consistent with the presence of high-spin ferric sites surrounded by an octahedron of oxygen atoms.[35] Furthermore, for a

(33) Pannetier, G.; Manoli, J. M.; Herpin, P. *Bull. Soc. Chim. Fr.* **1972**, *2*, 485.

(34) Loukili, M.; Durand, J.; Cot, L.; Rafiq, M. *Acta Crystallogr.* **1988**, *C44*, 6.

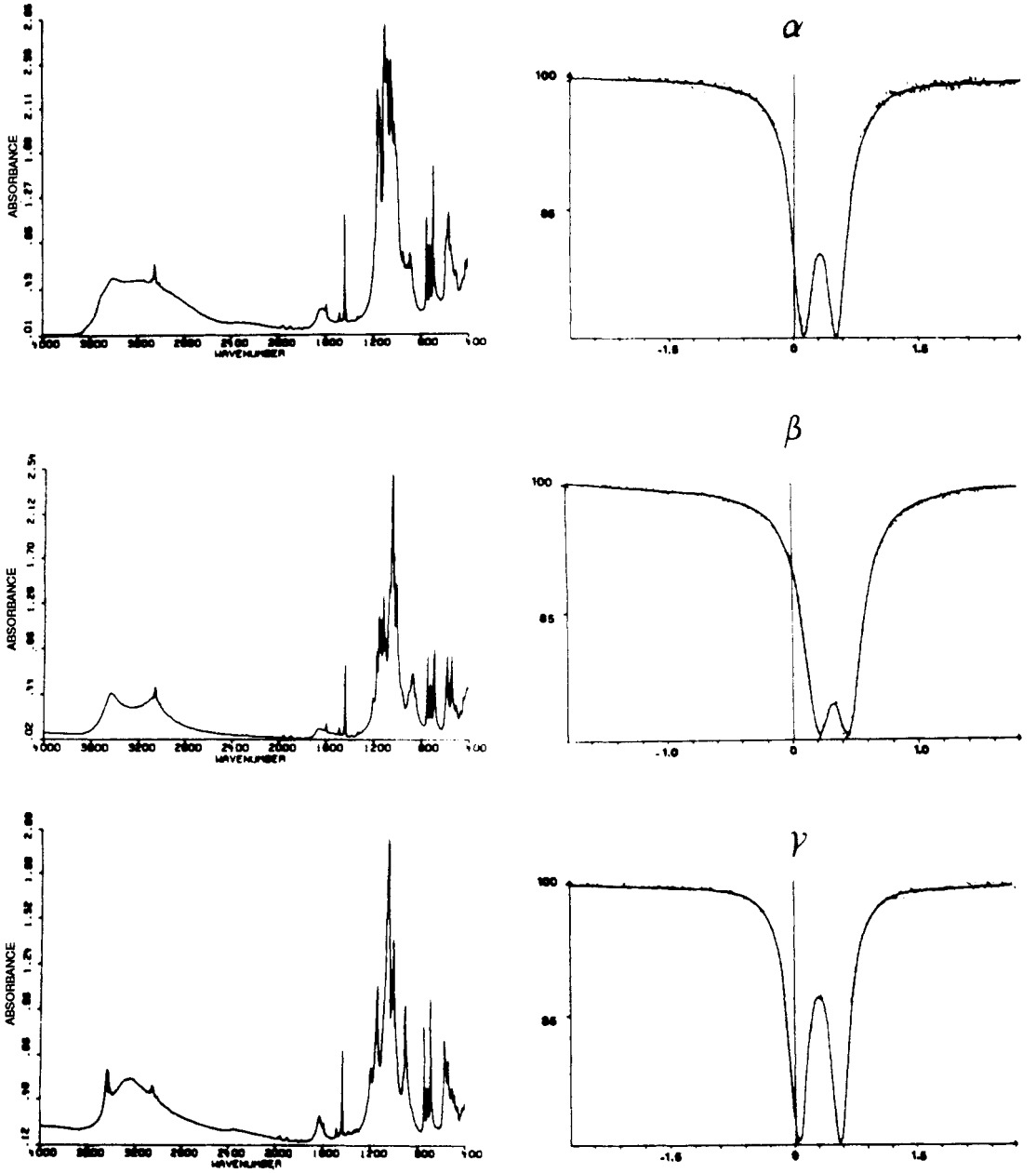

Figure 5. Room-temperature Mössbauer (relative absorption versus velocity (mm/s)) and infrared spectra of α, β, and γ.

powder sample of phase α, the reciprocal susceptibility as a function of temperature follows a Curie–Weiss law between 15 and 300 K, and the deduced magnetic moment is 6.0 μ_B, close to the spin-only value of 5.92 μ_B expected for independent $S = {}^5/_2$ ions. On the other hand, the presence of somewhat different quadrupole splittings for the three compounds (QS(α) = 0.40, QS(β) = 0.25, QS(γ) = 0.51 mm/s) gives evidence for differences in the electronic environment of the iron atom. However, the symmetry of the metallic site is greater than in FeOCl (QS = 0.97 mm/s) since the metal is now bonded to six oxygens. The main differences between the infrared spectra of α, β, and γ are observed in the PO_3 groups vibration domain (1000–1200 cm^{-1}) as well as in the O–H stretching vibration domain (3000–3500 cm^{-1}), but they do not allow us to draw meaningful conclusions regarding the structures. Finally a detailed study of these phases was carried out via TGA and DTA measurements. Representative curves are the same for compounds α, β, and γ with identical weight losses (Figure 6).

Three weight losses accompanied by endothermic peaks were observed at 200, 300, and 495 °C, respectively. The thermogravimetry unit was coupled to a mass spectrometer in order to identify the emitted gas at the successive stages (Figure 7), leading to the following assignments: 200 °C, weight loss 4.7%, 18 g per formula weight, emitted gas water, compound formed $HFe(C_6H_5PO_3)_2$; 300 °C, weight loss 2.4%, 9 g per formula weight, emitted gas water, resulting compound $Fe_2P_4O_{11}(C_6H_5)_4$; 495 °C, the weight loss corresponds to the degradation of the organic moiety since the emitted gas was benzene but is difficult to quantify. In fact, carbon was observed to deposit on the surface of the sample during decomposition.

If the analyses were carried out under air gas flow, the decomposition temperatures were not shifted, but no formation of carbon was observed due to an oxidation of the decomposition products of the sample. The weight loss was then 35.4% (137 g per formula weight), and the resulting compound was $Fe_2P_4O_{13}$. Mössbauer spectroscopy

(35) Menil, F. *J. Phys. Chem. Solids* **1985**, *46*, 763.

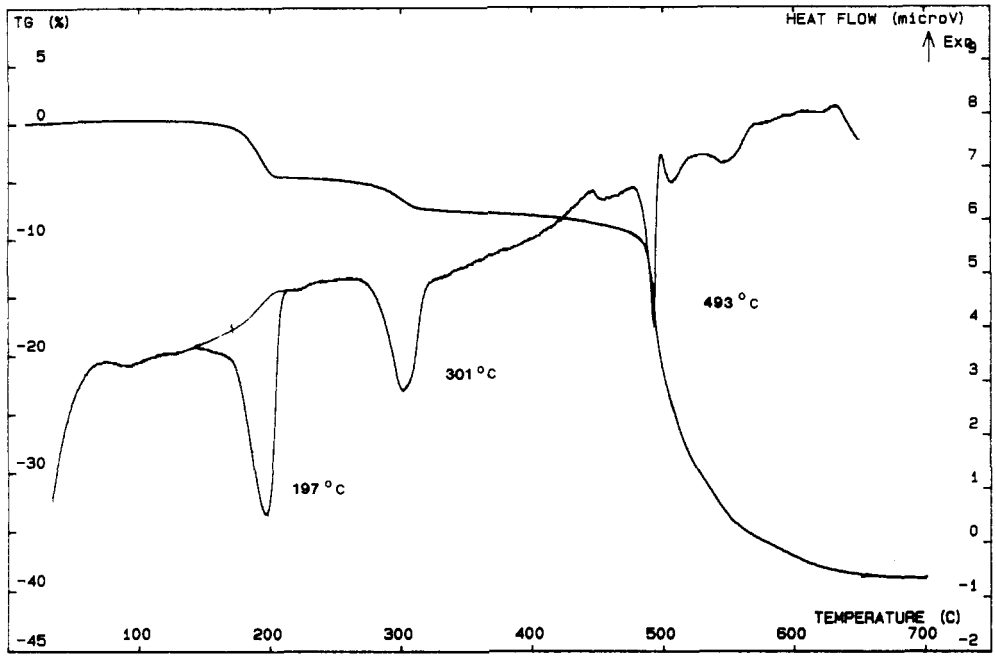

Figure 6. Thermogravimetric analysis curve for the α-phase.

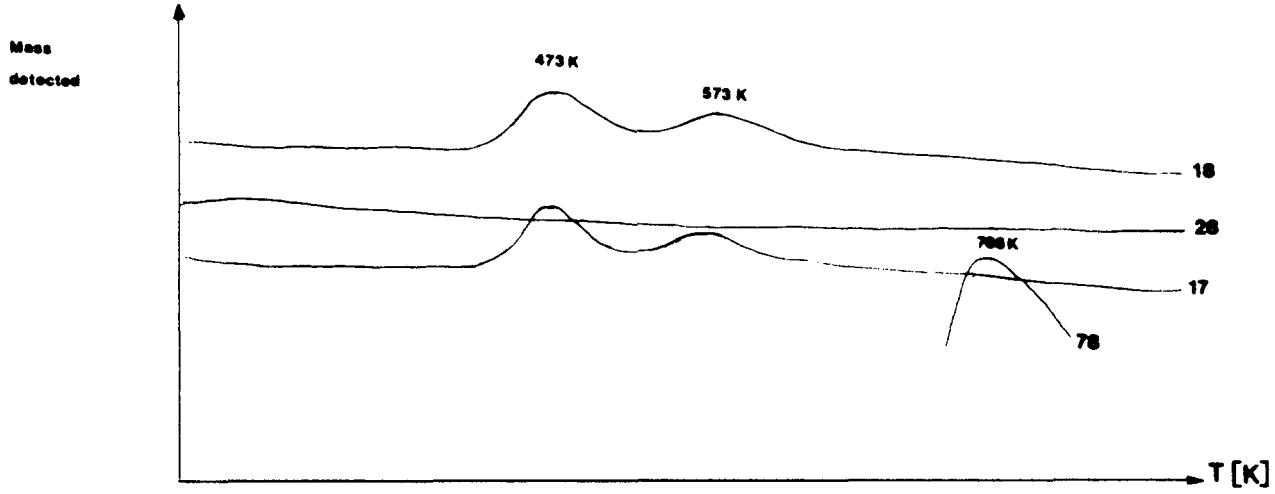

Figure 7. Analysis by mass spectrometry of the emitted gas as a function of temperature.

showed that the residue still had Fe^{3+} and the oxidation state of phosphorus atoms passed from 3^+ to 5^+ while a homolytic P–C bond scission occurred.[12a] Infrared spectra revealed that the characteristic vibrations of the phenyl ring were absent.

As we studied the compound $HFe(C_6H_5PO_3)_2$ obtained after the first water loss at 200 °C, we observed that it was characterized by the same IR, X-ray, and Mössbauer spectra, independent of the starting material (α, β, or γ). The three structures would then differ principally in their interlayer structural arrangement, that is, in the location of the water molecule.

For α, β, and γ, the low variation in the basal spacing (d = 14.61 Å) during dehydration, the differences in the O–H stretching vibration and PO_3 vibration domains in the infrared spectra, and the nonidentical quadrupole splittings are consistent with a location of the water molecule relatively near the metallic nucleus. The shortest $Fe–H_2O$ distance likely corresponds to the largest quadrupole splitting, but Fe K-edge EXAFS measurements would be necessary to make a more definite assignment.

It is noted that, on prolonged refluxing, $HFe(C_2H_5PO_3)_2·H_2O$ (obtained starting with ethylphosphonic acid) leads to a lamellar derivative whose structural determination shows that the water molecule is directly fixed to the iron atom.[36] This fact supports the idea that, in the case of $HFe(C_6H_5PO_3)_2·H_2O$, the water molecule is close to the Fe atom but does not succeed in bonding to it, probably due to steric hindrance.

These results also suggest that chemical processes that modify the structure of the FeOCl inner layer itself can occur, whereas this structure remained unchanged during the intercalation and the topotactic grafting reactions previously described.[19c,20] During the reaction of phenylphosphonic acid with FeOCl, a dissolution of the layered material probably takes place with reprecipitation of the crystalline iron phosphonates. The reaction process probably consists in an intercalation step (noticed with other phosphonic acids actually studied) followed by a substitution of the chlorine atoms via the phosphoryl group with a concomitant breakdown of the Fe–O–Fe network by the conjugated action of the OH groups and the HCl eliminated during the reaction. Thus, we have examined

(36) Bujoli, B.; Palvadeau, P.; Rouxel, J. *C. R. Acad. Sci. Paris*, submitted.

the possibility of obtaining the same complexes starting from other Fe materials such as α-Fe_2O_3, $FeCl_3$, and hydrated $Fe_2(SO_4)_3$. Following the same procedure as the one described for the synthesis of the α-phase in acetone, $FeCl_3$ (homogeneous medium) and hydrated $Fe_2(SO_4)_3$ (heterogeneous medium) led to the α-phase in 40% and 80% yield, respectively. No reaction was observed starting from α-Fe_2O_3. The conclusion is that the layered nature of FeOCl is not actually necessary for this synthesis. Nevertheless this study is a contribution to the identification and the preparation of new ironphosphonates.

Work is currently in progress to extend the synthetic chemistry of derivatized layered ironphosphonates via FeOCl, by studying the effects of the substituents borne by various phosphonic acids (R = alkyl, carboxylic acids, alcohol, etc.) and the possibility of making specific organic reactions in their interlayer space, especially when functional organic groups are bound to phosphorus.

Acknowledgment. We acknowledge the Commission of European Communities for support of this work under Grant No. MA1E-0030-C.

Registry No. I, 128752-87-4; II, 72702-16-0; FeOCl, 13870-10-5; $FeCl_3$, 7705-08-0; $Fe_2(SO_4)_3$, 10028-22-5.

Supplementary Material Available: Tables of anisotropic thermal parameters, positional parameters for hydrogen atoms, and a complete list of bond lengths and angles (3 pages); final observed and calculated structure factors (4 pages). Ordering information is given on any current masthead page.

Growth and Characterization of Gallium Arsenide Using Single-Source Precursors: OMCVD and Bulk Pyrolysis Studies

James E. Miller,[1a] Kenneth B. Kidd,[1b] Alan H. Cowley,*[,1b] Richard A. Jones,*[,1b] John G. Ekerdt,[1a] Henry J. Gysling,*[,1c] Alex A. Wernberg,[1c] and Thomas N. Blanton[1d]

Departments of Chemical Engineering and Chemistry, The University of Texas at Austin, Austin, Texas 78712, and Corporate Research Laboratories and Analytical Technology Division, Eastman Kodak Company, Rochester, New York 14650

Received March 12, 1990

Films of gallium arsenide have been grown on GaAs(100), GaAs(111), and α-Al_2O_3(0001) at 1×10^{-4} Torr and 525 °C by using a single-source precursor $[Me_2Ga(\mu\text{-}t\text{-}Bu_2As)]_2$ (1) and H_2 carrier gas. These conditions resulted in GaAs growth rates of 0.75 μm/h. The carbon content of the films was less than the XPS detection limit (1000 ppm). Secondary ion mass spectrometry (SIMS) revealed that carbon was not incorporated from the precursor. Photoluminescence spectra (5 K) of the material grown on α-Al_2O_3(0001) exhibited the 1.52-eV bandgap of GaAs. However, the material appears degeneratively doped. X-ray diffraction, Berg–Barrett topography, and pole figure analysis indicated that these GaAs films are (111) orientated and polycrystalline. Mass spectroscopic analysis of the OMCVD reaction of 1 revealed that the volatile products are predominantly isobutylene and methane. Bulk pyrolysis studies demonstrated that at lower temperatures (350 °C) the decomposition of 1 is incomplete and that isobutane is produced in addition to isobutylene and methane. Under similar conditions, the decomposition of $[n\text{-}Bu_2Ga(\mu\text{-}t\text{-}Bu_2As)]_2$ (2) is virtually complete. The thermolysis of 2 produced isobutane (60%), isobutylene (32%), *n*-butane (9.6%), 1-butene (44%), *trans*-2-butene (26%), and *cis*-2-butene (19%).

Introduction

Organometallic chemical vapor deposition (OMCVD) has become a leading technique for producing epitaxial films of group III–V compound semiconductors. Typically, OMCVD processes employ a group III trialkyl such as Me_3Ga and a group V hydride such as AsH_3. Reaction of the group III and V sources in the temperature range 600–700 °C results in the desired semiconducting films.[2] However, despite its widespread use the conventional OMCVD method suffers from a number of drawbacks. The high toxicity of AsH_3 and the pyrophoric nature of the group III alkyls represent health, safety, and environmental hazards.[2-8] Other problems that have been encountered include carbon contamination and prereactions, particularly in the case of InP growth. Furthermore, it is desirable to lower the deposition temperatures to minimize the interdiffusion of layers and dopants. Various attempts have been made to address these problems. For example, modifications to the conventional OMCVD have been developed, and the use of alternative group V and to a lesser extent group III sources have been investigated.[9-18] An interesting alternative approach has been to

(1) (a) Department of Chemical Engineering, UT Austin. (b) Department of Chemistry, UT Austin. (c) Corporate Research Laboratories, Eastman Kodak Company. (d) Analytical Technology Division, Eastman Kodak Company.

(2) Ludowise, M. J. *J. Appl. Phys.* **1985**, *58*, R31.
(3) Lum, R. M.; Klingert, J. K.; Dutt, B. V. *J. Cryst. Growth* **1986**, *75*, 421.
(4) Shastry, S. K.; Zemon, S.; Kenneson, D. G.; Lambert, G. *Appl. Phys. Lett.* **1988**, *52*, 150.
(5) Kuech, T. F.; Veuhoff, E. *J. Cryst. Growth* **1984**, *68*, 148.
(6) Stringfellow, G. B. *J. Cryst. Growth* **1986**, *75*, 91.
(7) Bradley, D. C.; Faktor, M. M.; Scott, M.; White, E. A. D. *J. Cryst. Growth* **1986**, *75*, 101.
(8) Moss, R. H. *J. Cryst. Growth* **1984**, *68*, 78.
(9) Larsen, C. A.; Chen, C. H.; Kitamura, M.; Stringfellow, G. B.; Brown, D. W.; Robertson, A. J. *Appl. Phys. Lett.* **1986**, *48*, 1531.
(10) Kurtz, S. R.; Olson, J. M.; Kibbler, A. *J. Electron. Mater.* **1989**, *18*, 15.
(11) Kellert, F. G.; Whelan, J. S.; Chan, K. T. *J. Electron. Mater.* **1989**, *18*, 355.

0897-4756/90/2802-0589$02.50/0